

Animal Model

Regulation of Local Host-Mediated Anti-Tumor Mechanisms by Cytokines

Direct and Indirect Effects on Leukocyte Recruitment and Angiogenesis

Morihiro Watanabe,* Kathryn L. McCormick,[†]
Kirk Volker,[†] John R. Ortaldo,*
Jon M. Wigginton,* Michael J. Brunda,[‡]
Robert H. Wiltrout,* and William E. Fogler*

From the Laboratory of Experimental Immunology, Division of Basic Sciences and Intramural Support Research Program, SAIC Frederick,[†] National Cancer Institute-Frederick Cancer Research and Development Center, Frederick, Maryland, and the Department of Oncology,[‡] Hoffmann-La Roche, Nutley, New Jersey*

The regulation of tumor growth by cytokine-induced alterations in host effector cell recruitment and activation is intimately associated with leukocyte adhesion and angiogenic modulation. In the present study, we have developed a novel tumor model to investigate this complex series of events in response to cytokine administration. Gelatin sponges containing recombinant human basic fibroblast growth factor (rhFGFb) and B16F10 melanoma cells were implanted onto the serosal surface of the left lateral hepatic lobe in syngeneic C57BL/6 mice. The tumor model was characterized by progressive tumor growth initially localized within the sponge and the subsequent development of peritoneal carcinomatosis. Microscopic examination of the sponge matrix revealed well developed tumor-associated vascular structures and areas of endothelial cell activation as evidenced by leukocyte margination. Treatment of mice 3 days after sponge implantation with a therapeutic regimen consisting of pulse recombinant human interleukin-2 (rhIL-2) combined with recombinant murine interleu-

kin-12 (rmIL-12) resulted in a marked hepatic mononuclear infiltrate and inhibition of tumor growth. In contrast to the control group, sponges from mice treated with rhIL-2/rmIL-12 demonstrated an overall lack of cellularity and vascular structure. The regimen of rhIL-2 in combination with rmIL-12 was equally effective against gelatin sponge implants of rhFGFb/B16F10 melanoma in SCID mice treated with anti-asialo-GM1 in the absence of a mononuclear infiltration, suggesting that T, B, and/or NK cells were not the principal mediators of the anti-tumor response in this tumor model. The absence of vascularity within the sponge after treatment suggests that a potential mechanism of rhIL-2/rmIL-12 anti-tumor activity is the inhibition of neovascular growth associated with the establishment of tumor lesions. This potential mechanism could be dissociated from the known activities of these two cytokines to induce the recruitment and activation of host effector cells. Moreover, this model provides a unique opportunity to study the cellular and molecular mechanism(s) underlying both tumor angiogenesis and leukocyte recruitment to metastatic lesions. (Am J Pathol 1997, 150:1869–1880)

Accepted for publication February 6, 1997.

Address reprint requests to Dr. William E. Fogler, Experimental Therapeutics Section, Laboratory of Experimental Immunology, Division of Basic Science, NCI-FCRDC, Building 560, Room 31-93, Frederick, MD 21702-1201.

The progressive growth of primary neoplasms and metastatic lesions is dependent on angiogenesis¹ and is often associated with inflammatory processes resulting in the recruitment and subsequent infiltration of the tumor by host leukocytes.² A principal pathway of leukocyte infiltration of metastatic lesions is thought to involve a sequential series of events whereby leukocytes initially adhere to the tumor vasculature with subsequent transmigration in response to specific cytokines and/or chemokines.³⁻⁷ The relationship between the neovascular network of the tumor microenvironment and leukocyte recruitment has formed the basis of many therapeutic strategies using systemically administered recombinant cytokines and/or adoptively transferred, *ex vivo* activated effector cells (reviewed in Ref. 8). These therapeutic strategies have attempted to facilitate leukocyte recruitment from the vascular compartment to tumor-involved organ parenchyma and metastatic lesions through the induction or augmentation of specific physiological signals. Inherent in these strategies has been the tenet that leukocyte/endothelial adhesion and transmigration are requisite events for successful biological therapy of cancer. Relatively little attention has been given to the relationship and relative contributions of leukocyte recruitment and neovascularization to anti-tumor responses.

The process of tumor angiogenesis *in vivo* is regulated both by angiogenic stimulators such as fibroblast growth factors (FGFs) and vascular endothelial growth factor (VEGF)⁹⁻¹³ and by angiogenic inhibitors such as thrombospondin and angiostatin.¹⁴⁻¹⁶ Several lines of evidence have now suggested direct links between leukocyte/endothelial interaction and neoplastic vascular development. The cytokine-inducible, endothelial adhesion molecules, E-selectin and vascular cell adhesion molecule-1 (VCAM-1) mediate the rolling and firm adhesion phase, respectively, of specific leukocyte subsets.³⁻⁶ These adhesion ligands in soluble form have also been recently reported to induce chemotaxis of endothelial cells *in vitro* and to promote neovessel growth in the rat cornea.¹⁷ Moreover, recent *in vitro* studies have also suggested that the angiogenic stimulators FGF and VEGF directly regulate VLA-4- and LFA-1/Mac-1-dependent binding of natural killer (NK) cells to endothelium.¹⁸ In addition, subfamilies of the C-X-C chemokines that stimulate the chemotactic transmigration of distinct sets of leukocytes can also directly regulate the process of angiogenesis.¹⁹ Studies have shown interleukin-8 (IL-8) to promote neovessel growth^{20,21} whereas *gro-β* and the interferon-inducible protein 10 (IP-10) inhibit

angiogenesis.^{22,23} Collectively, these studies suggest that the regulation of tumor growth by cytokine-induced alterations in host effector cell recruitment and activation is intimately associated with leukocyte adhesion and angiogenic modulation.

A number of experimental models have been developed to facilitate the *in vivo* study of leukocyte recruitment and to elucidate critical determinants that may impact either directly or indirectly the treatment of metastatic tumor growth.²⁴⁻²⁸ Although these models have provided important qualitative and quantitative information on leukocyte trafficking to tumors, they have not been well suited for concomitant determinations of angiogenic modulation. Similarly, models of tumor angiogenesis, such as the corneal micropocket assay^{21,29} or those incorporating Matrigel implantation,^{30,31} have not been exploited to study the regulation of leukocyte recruitment. With the parallel development of data implicating complementary interactions between cytokine-induced leukocyte recruitment and the direct development of tumor neovasculation, the development of tumor models capable of simultaneously addressing both aspects is warranted.

Recently, we have described the use of FGF-adsorbed gelatin sponges affixed to various murine peritoneal tissues to generate organ-derived vascular beds.³² This technique allowed a generalized method for the recovery and culture of tissue-specific endothelium and permitted the *in vitro* study of leukocyte/endothelial cell interactions.³² As originally reported, the use of implanted FGF-adsorbed gelatin sponges was developed as a model to permit the molecular dissection of the *in vivo* physiological mechanisms that control neovascularization.³³ The adsorption strategy induced a rapid vascular development at the organ-specific site that was accompanied by leukocyte infiltration and was able to sustain the survival and proliferative potential of a rat hepatocyte cell line simultaneously implanted with the FGF-treated sponges.³³ Subsequent studies employing gelatin sponge implants lacking FGF but containing irradiated tumor cells have been used to define factors that govern the recruitment and activation of tumor-specific lymphocytes during the development of an anti-tumor response.³⁴

In the present study, we report on the development of a novel tumor model using recombinant human basic FGF (rhFGFb)-adsorbed gelatin sponges containing the B16F10 melanoma, which were affixed to the livers of syngeneic C57BL/6 mice. Using this model, we have studied the relationship between the induction of hepatic leukocyte infiltra-

tion, local angiogenic modulation, and anti-tumor activity after treatment of mice with a previously defined therapeutic regimen consisting of recombinant murine interleukin-12 (rmIL-12) in combination with pulse recombinant human interleukin-2 (rhIL-2).³⁵ The results suggest that this model provides a unique opportunity to study the cellular and molecular mechanism(s) underlying the recruitment of leukocytes to metastatic lesions and tumor angiogenesis.

Materials and Methods

Mice

Specific-pathogen-free C57BL/6 and B6 *scid/scid* (SCID) mice (8 to 12 weeks of age) were obtained from the Animal Production Area, NCI-Frederick Cancer Research and Development Center (Frederick, MD). Mice were kept under specific-pathogen-free conditions and provided sterilized mouse chow (Ziegler Bros., Gardner, PA) and water *ad libitum*. SCID mice were housed in microisolator cages and also received 40 mg of trimethoprim and 200 mg of sulfamethoxazole per 320 ml of drinking water. Animal care was provided in accordance with the procedures outlined in the Guide for the Care and Use of Laboratory Animals (National Institutes of Health Publication 86-23, 1985).

Reagents

rhIL-2 (Tecin; 3.2×10^7 U/mg) and rmIL-12 (7×10^6 U/mg) were provided by Hoffmann-La Roche (Nutley, NJ). Stock aliquots of rmIL-12 in sterile $\text{Ca}^{2+}/\text{Mg}^{2+}$ -free Dulbecco's phosphate-buffered saline (PBS) were stored at -70°C until use. For *in vivo* administration, the stock solutions were diluted as necessary with PBS containing 0.1% sterile-filtered B6 mouse serum and used within 48 hours. rhFGFb was obtained from PeproTech (Rocky Hill, NJ) and stored as aliquots at -70°C in 50 mmol/L Tris/HCl, pH 7.4, until use. Rabbit anti-asialo-GM1 antisera was purchased from WAKO Chemicals USA (Richmond, VA).

Cell Culture

The murine melanoma cell line B16F10 syngeneic to C57BL/6N mice was provided by Dr. Isaiah Fidler (Houston, TX). Cells were grown as monolayer cultures and were maintained in Dulbecco's minimal essential medium containing 5% heat-inactivated fetal calf serum, 4 mmol/L L-glutamine, and 2 mmol/L

sodium pyruvate. The cells were passaged when the cultures were approximately 80% confluent and used between 6 and 18 passages.

Hepatic Implantation of rhFGFb- Impregnated Sponges Containing B16F10 Melanoma

Hepatic implants of vascularized gelatin sponges containing progressively growing B16F10 melanoma cells were generated using a modification of previously published techniques.^{32,33} Sterile Gelfoam sponges (Upjohn, Kalamazoo, MI) were cut into squares of approximately $5 \times 5 \times 5$ mm (125 mm^3), hydrated, and de-aerated in sterile PBS overnight. The sponges were then blotted dry and equilibrated in 50 mmol/L Tris/HCl, pH 7.4, for 60 minutes at 37°C . After equilibration, the sponges were again blotted dry and incubated for 60 minutes at 37°C with $85 \mu\text{l}$ of 50 mmol/L Tris/HCl (pH 7.4) containing $1.25 \mu\text{g}$ of rhFGFb.

Cultures of B16F10 melanoma cells in exponential growth phase were harvested by a short trypsinization (0.25% trypsin and 0.02% EDTA for 1 minute at 37°C), washed, and resuspended to 2×10^7 cells/ml in $\text{Ca}^{2+}/\text{Mg}^{2+}$ -free Hanks' balanced salt solution (HBSS). Ten microliters of the cell suspension (2×10^5 cells) were added directly to each individual sponge containing $125 \mu\text{g}$ of rhFGFb before implantation onto the livers of mice.

Individual B6 or B6 SCID mice were anesthetized with methoxyflurane (Pitman-Moore, Mundelein, IL), and the abdomens were washed with 70% ethanol. An incision was made along the midline of the abdomen to expose the abdominal cavity. A sponge, prepared as described above, was affixed to the serosal surface of the left lateral hepatic lobe using cyanoacrylate adhesive. The margins of the surgical incision were then approximated and closed with Clay Adams 9-mm autoclips.

Treatment of Hepatic Sponge Implants with rmIL-12 in Combination with Pulse rhIL-2

Cohorts of six to eight hepatic sponge-implanted B6 mice were used for all treatment groups and were administered rmIL-12 in combination with pulse rhIL-2 as previously described.³⁵ Briefly, mice were given 300,000 IU of rhIL-2 intraperitoneally twice daily on days 3 and 10 after sponge implantation. rmIL-12 ($0.5 \mu\text{g}$), or PBS plus mouse serum vehicle alone, was administered by daily intraperitoneal injection on days 3 to 7 and 10 to 14. The identical

protocol was used to treat B6 SCID mice that had also received 0.1 ml of rabbit anti-asialo-GM1 antisera intravenously 3 days before and days 4 and 11 after sponge implantation to deplete NK cells.³⁶ B6 SCID mice were maintained on prophylactic antibiotics in their drinking water for the duration of all experiments.

Pathology

Three days after treatment, mice were necropsied and liver tissue with attached sponges were fixed in 10% neutral buffered formalin for 24 hours and then changed to 70% ethanol. Tissues were embedded in paraffin by routine methods, sectioned at 6 μm , and stained with hematoxylin and eosin (H&E) by the Pathology Histotechnology Laboratory, SAIC Frederick, NCI-FCRDC, Frederick, MD. Selected sections were stained with Masson's trichrome stain. Photomicrographs were obtained using an Olympus BH-2 microscope.

Isolation and Analysis of Hepatic Infiltrative Mononuclear Cells

Leukocytes were obtained from the livers of control and rML-12/pulse-rhIL-2-treated mice by a modification of previously described techniques.³⁷ Livers were first perfused with 25 ml of HBSS and excised. Cell suspensions were generated after a 2-minute disruption in a stomacher (Tekmar Co., Cincinnati, OH). The resulting cell suspensions were centrifuged at $500 \times g$ for 5 minutes, and the pellet was resuspended and filtered through 100- μm nylon mesh. The cellular filtrate was centrifuged at $500 \times g$ for 5 minutes, and the pellet was resuspended to 35 ml in HBSS. The cell suspension was then underlaid with 13 ml of Lympholyte-M (Cedar Lane Laboratories, Ontario, Canada) and centrifuged at $1400 \times g$ for 30 minutes at room temperature. After centrifugation, 10 ml of the interface was aspirated, mixed with 40 ml of HBSS, and centrifuged at $500 \times g$ for 5 minutes. The resulting cell pellet was resuspended in 0.2% bovine serum albumin in HBSS for two-color flow cytometric analysis (FCA) as described below.

Cells were labeled with optimally titrated antibodies, and cellular fluorescence was determined on 1.5×10^4 cells using a FACScan analyzer (Becton Dickinson, San Jose, CA). All antibodies used for FCA were obtained from PharMingen (San Diego, CA). T cells or NK cells were detected using fluorescein isothiocyanate (FITC)-labeled anti-CD3 (clone 145-2C11) or R-phycoerythrin-labeled anti-NK1.1

(clone PK136), respectively. CD4⁺ or CD8⁺ T cells were detected by using phycoerythrin-labeled anti-CD4 (clone H129.19) and FITC-labeled anti-CD8a (clone 53-6.7). B-lineage cells (mature and immature) were detected with phycoerythrin-labeled anti-B220 (clone RA3-6B2) and mature B cells were detected by using a FITC-labeled affinity-purified goat anti-mouse IgM (μ -H-chain specific) antibody (slg- μ -bearing, slgM⁺). Macrophage/myeloid cells were detected using FITC-labeled anti-MAC-1 (clone M1/70) and phycoerythrin-labeled anti-Gr-1/myeloid differentiation antigen (clone RB6-8C5). The data were analyzed by the use of FACScan research and LYSYS software programs written for the Hewlett Packard Consort 30 microcomputer integral to the FACScan analyzer (Becton Dickinson). The percentage of cells bearing a particular phenotypic marker was determined on a pool of five livers/group, and the number of cells bearing a particular marker was determined by multiplying this percentage by the mean of the total number of cells of the pooled livers.

Results

Growth of B16F10 in rhFGFb-Adsorbed Gelatin Sponge Hepatic Implants

Individual gelatin sponges containing an initial concentration of 1.25 μg of rhFGFb and 2×10^5 B16F10 melanoma cells was implanted onto the serosal surface of the left lateral hepatic lobe in ten B6 mice. Twenty days after implantation, mice were euthanized and examined for tumor growth. Progressive hepatic tumor growth was noted in all mice implanted with B16F10 cells in rhFGFb-adsorbed gelatin sponges. The tumors appeared as a melanotic lesion ranging in size from 8 to 15 mm in diameter at the site of implantation. Although the majority of the hepatic tumor mass was present as a single localized lesion, occasionally smaller tumors were noted within the same lobe or the left and/or right medial lobes. There was no evidence of pulmonary metastases, although studding of the peritoneal cavity with tumor foci was observed in all mice. Histological examination of the primary hepatic tumor mass showed well established vascular structures and evidence of endothelial activation as indicated by leukocyte margination and infiltration (Figure 1A). Cellular elaboration of extracellular matrix proteins circumscribed the vascular components and was evident throughout the tumor mass (Figure 1B).

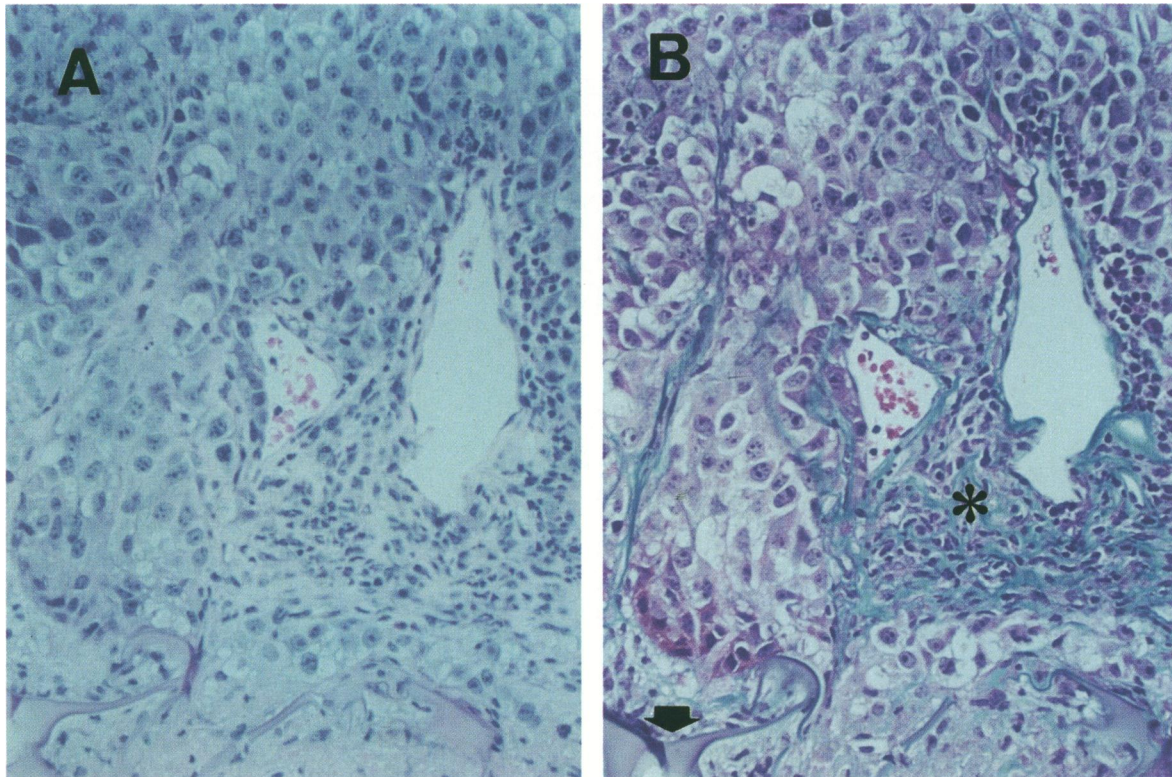


Figure 1. Vascular development and tumor growth within a *rbFGFb*-impregnated sponge implanted on the liver of a *C57BL/6* mouse (day 18). Original magnification, $\times 132$. **A:** H&E. **B:** Masson's trichrome, same field as shown in **A**. Note the deposition of extracellular matrix components and leukocyte infiltration (asterisk). Gelatin sponge fibers are also shown in the bottom of the field (arrow).

Anti-Tumor Activity of rmlL-12 and Pulse rhIL-2 against Hepatic Sponge Implants of B16F10 and rhFGFb

To begin to investigate the utility of this tumor model to study the relationship between the induction of hepatic leukocyte infiltration by cytokines, local angiogenic modulation, and anti-tumor activity, cohorts of six B6 mice were treated intraperitoneally with control diluent or two cycles of a previously described therapeutic regimen of *rmlL-12* in combination with *rhIL-2*,³⁵ beginning 3 days after hepatic implantation of gelatin sponges containing an initial concentration of $1.25 \mu\text{g}$ of *rhFGFb* and 2×10^5 B16F10 melanoma cells. Mice were euthanized 3 days after the final injection and examined for progressive tumor growth. At this time point, the mean sponge-associated tumor volume in control-treated mice was $784 \pm 101 \text{ mm}^3$ (Figure 2). In contrast, a substantial reduction in tumor volume to below measurable levels was observed in hepatic sponges from mice treated with *rmlL-12* and *rhIL-2* (Figure 2). In addition, although pronounced peritoneal carcinomatosis was observed in six of six mice treated with control diluent, four of six mice treated with *rmlL-12*

and *rhIL-2* were macroscopically free of extrahepatic tumor growth (data not shown).

Microscopic examination of the interface between the sponge and hepatic parenchyma from control diluent-treated mice 3 days after the final injection showed localized tumor growth and hypervascular development within the sponge matrix with minimal leukocyte infiltration (Figure 3A). In contrast, rela-

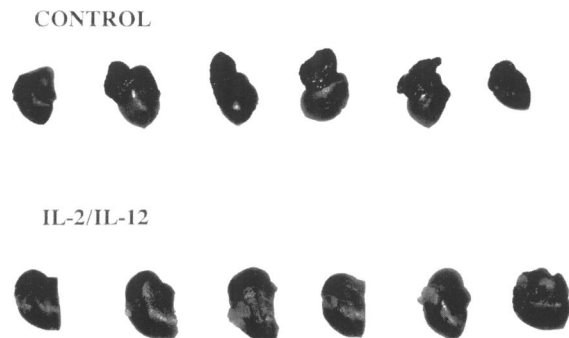


Figure 2. Hepatic *rbFGFb*-impregnated sponges and B16F10 tumor burden (day 22) from *C57BL/6* mice treated with control diluent (top) or *rmlL-12* and pulse *rhIL-2* (bottom). In control-treated mice, a progressively growing melanoma is localized within the hepatic sponge. Little or no tumor growth is observed within the sponges from mice treated with *rmlL-12* and pulse *rhIL-2*.

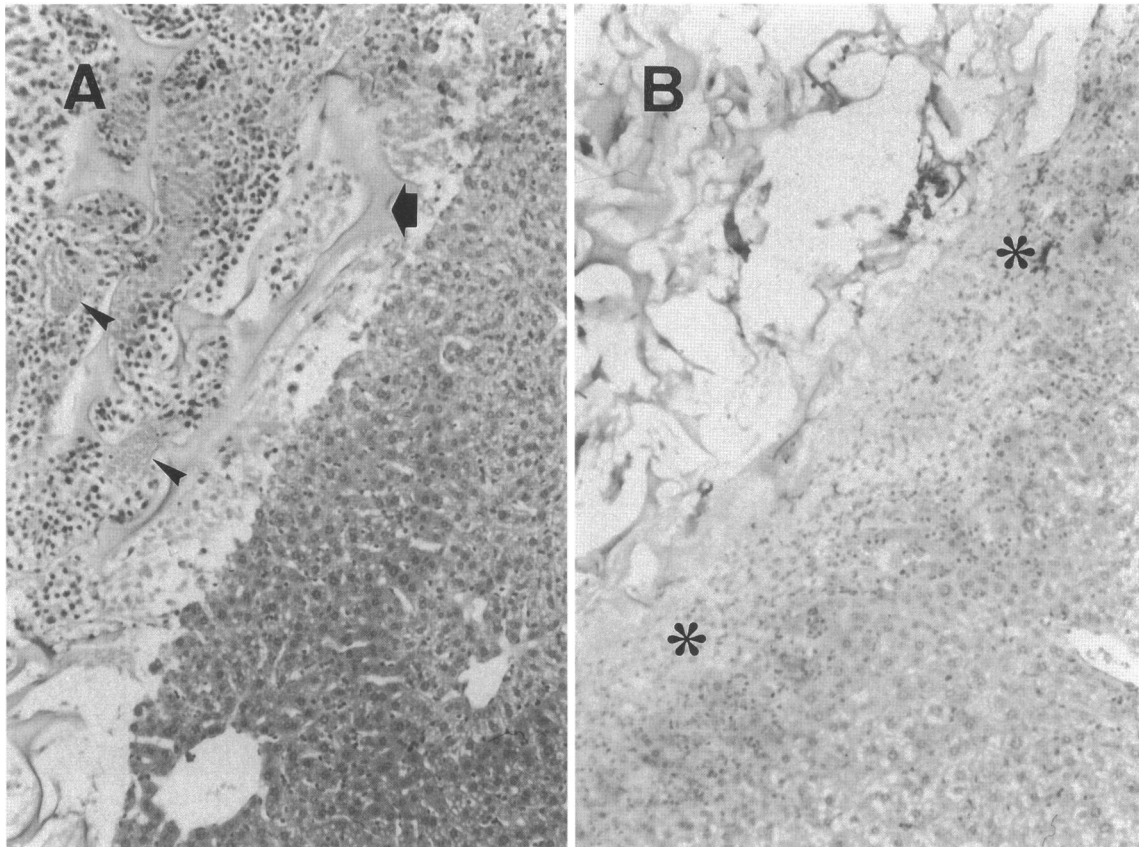


Figure 3. Interface between *rbFGF* sponge/B16 melanoma liver implant and hepatic tissue (day 22) from tumor-bearing mice treated with control diluent (A) or *rmlL-12* and pulse *rhIL-2* (B). H&E, original magnification, $\times 66$. Within the gelatin sponge matrix (arrows) of control-treated mice are numerous vascular structures (arrowheads) and tumor cells. In contrast, there is an acellularity within the sponge of mice treated with *rmlL-12* and pulse *rhIL-2*, and a prominent leukocytic infiltration is observed at the sponge/liver interface (asterisks).

tively few tumor cells and no vascular structures were detected in sponges from mice treated with *rmlL-12* and *rhIL-2*, and a pronounced leukocyte infiltrate was apparent at the sponge/liver interface (Figure 3B). The absence of neovessel formation in the sponges was confirmed in multiple sections. An intense leukocyte infiltration was also observed in proximity to central veins and terminal portal venules within the hepatic parenchyma of sponge-implanted mice treated with *rmlL-12* and *rhIL-2* (Figure 4B) that was not apparent in mice treated with control diluent (Figure 4A).

Characterization of the Hepatic Leukocyte Infiltration Induced by rmlL-12 and rhIL-2

To determine the cellular composition and kinetics of this pronounced cytokine-induced infiltrate, cohorts of five B6 mice were injected intraperitoneally with control diluent or *rmlL-12* in combination with *rhIL-2* and livers were processed on days 1, 3, and 5 of treatment for the *ex vivo* determination of leukocyte

infiltration by FCA. Under these experimental conditions, *rmlL-12* and *rhIL-2* induced a significant time-dependent increase in hepatic leukocyte infiltration (ninefold; $P < 0.01$; Table 1). FCA demonstrated both cytokine-dependent ($NK1.1^+$, $CD3^+$, $8C5^+$, or $MAC-1^+$) and -independent ($B220^+$ or $sIgm^+$) alterations in the percentage of liver-infiltrating leukocytes. Overall, the infiltrate was characterized by an initial rapid influx and then loss of $NK1.1^+$ leukocytes and a concomitant increase of all other mature leukocyte populations by 10- to 35-fold depending on the subset (Table 1).

Anti-Tumor Activity of rmlL-12 and Pulse rhIL-2 against Hepatic Sponge Implants of B16F10 and rhFGFb in B6 SCID Mice

Given the marked alterations of hepatic leukocyte infiltration by *rmlL-12* and *rhIL-2*, we hypothesized that these potential anti-tumor effector cells were either directly or indirectly involved in the inhibition of

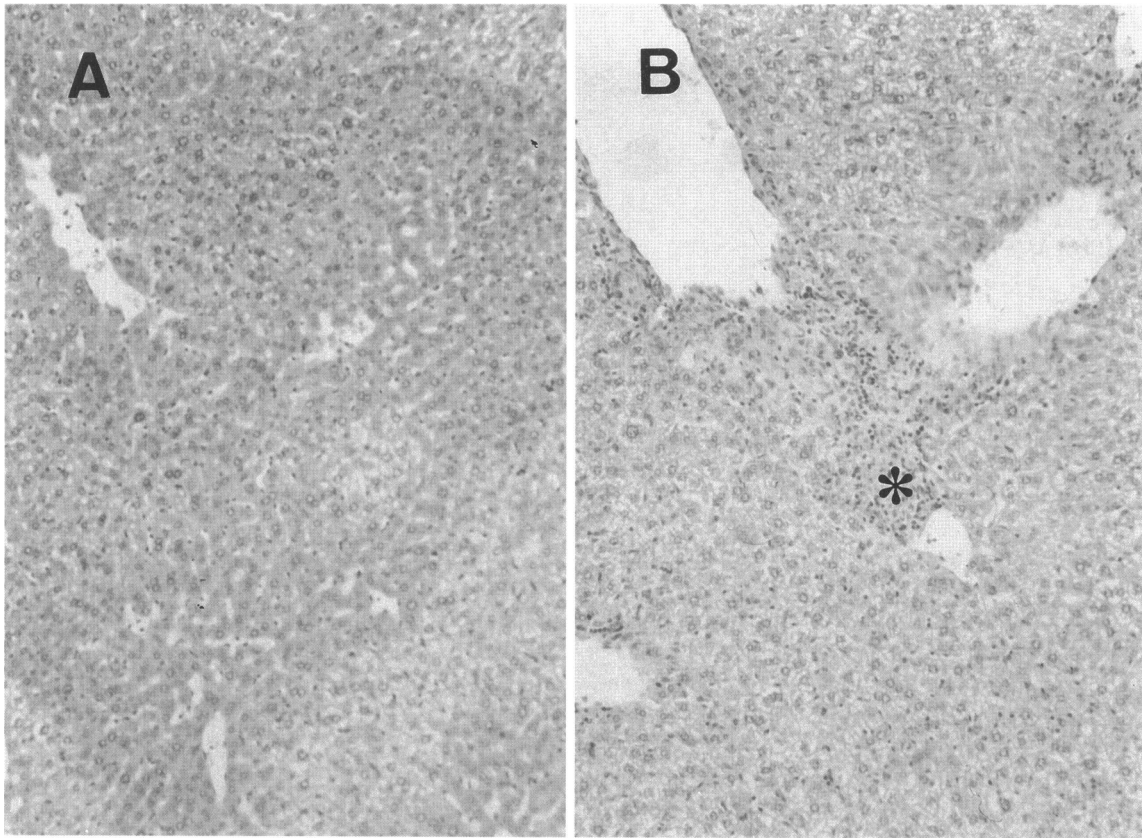


Figure 4. Liver parenchyma from rhFGFb sponge/B16 melanoma liver-implanted mice (day 22) treated with control diluent (A) or rmlL-12 and pulse rhIL-2 (B). H&E; original magnification, $\times 66$. Leukocyte infiltration is evident within the hepatic tissue of mice treated with rmlL-12 and pulse rhIL-2 (asterisk).

B16F10 tumor growth in the rhFGFb-treated sponge. To test this hypothesis, the therapy experiment was repeated in immune-competent B6 mice and in T- and B-cell-deficient B6 SCID mice treated with anti-asialo-GM1 to deplete NK cells.³⁶ Mice were euthanized 1 week after the final injection and examined for progressive tumor growth. No B6 SCID mice were lost to experimental techniques, and progressive hepatic tumor growth was noted in all mice implanted with B16F10 cells (Figure 5). Surprisingly, in comparison with B6 SCID mice treated with anti-asialo-GM1 and control diluent, a substantial reduction in tumor volume was observed in hepatic sponges from immune-compromised mice treated with rmlL-12 and

rhIL-2 (Figure 5). The reduction in tumor volume was equivalent to that observed in immune-competent mice identically treated (data not shown).

In agreement with the micropathology results shown in Figure 3B, relatively few tumor cells and no vascular structures were detected in sponges from immune-competent B6 mice treated with rmlL-12 and rhIL-2, and a pronounced leukocyte infiltrate was apparent at the sponge/liver interface (Figure 6A). In contrast, although there was a comparable absence of melanoma cells and endothelium in cytokine-treated, immune-compromised B6 SCID mice, this was associated with a minimal and discontinuous cellular infiltrate (Figure 6B). This his-

Table 1. Characterization of Hepatic Leukocyte Infiltrate Induced by rmlL-12 and rhIL-2

Treatment group	Total leukocytes/ liver ($\times 10^*$)	Percentage of total leukocytes positive for: [†]					
		NK1.1	CD3	B220	sIg μ	8C5	MAC-1
Control diluent	2.6	13	45	18	20	3	15
rhIL-2/rmlL-12 $\times 1$	6.1	31	22	20	19	5	39
rhIL-2/rmlL-12 $\times 3$	12.1	5	48	20	24	12	20
rhIL-2/rmlL-12 $\times 5$	23.4	1	51	22	25	12	20

*Results are expressed as the mean determination from five livers/treatment group. Variation from the mean did not exceed 15%.
[†]FCA was performed on pooled samples from each indicated group.

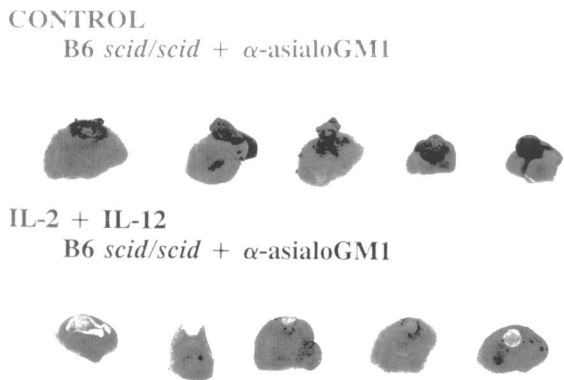


Figure 5. Hepatic *rbFGFb*-impregnated sponges and B16F10 tumor burden (day 19) from B6 SCID mice treated with α -asialo-GM1 and control diluent (top) or *rmIL-12* and pulse *rhIL-2* (bottom). Little or no tumor growth is observed within the sponges from mice treated with *rmIL-12* and pulse *rhIL-2*.

topathological profile was confirmed in multiple sections. Masson trichrome analysis of the sponge from *rmIL-12*- and *rhIL-2*-treated, NK-cell-depleted, B6 SCID mice showed, in addition to an overall acellularity, the absence of extracellular matrix protein deposition (Figure 7). These results suggested that a

potential mechanism of the anti-tumor activity observed with *rmIL-12* and *rhIL-2* treatment in this model may have resulted from the inhibition of sponge neovascularization leading to tumor cell death, which can be dissociated from the known activities of these two cytokines to induce the recruitment and activation of host effector cells. Moreover, in general, this model provides a unique opportunity to study the cellular and molecular mechanisms underlying both tumor angiogenesis and the recruitment of leukocytes to malignant lesions and the relative contributions of each to anti-tumor effects induced by various types of biological therapy.

Discussion

In the present study, we have developed a novel hepatic tumor model to investigate cytokine-induced alterations in host effector cell recruitment and tumor angiogenesis. The model is predicated on the ability of gelatin to bind the angiogenic stimulus FGF and, after implantation into mice, to induce the rapid for-

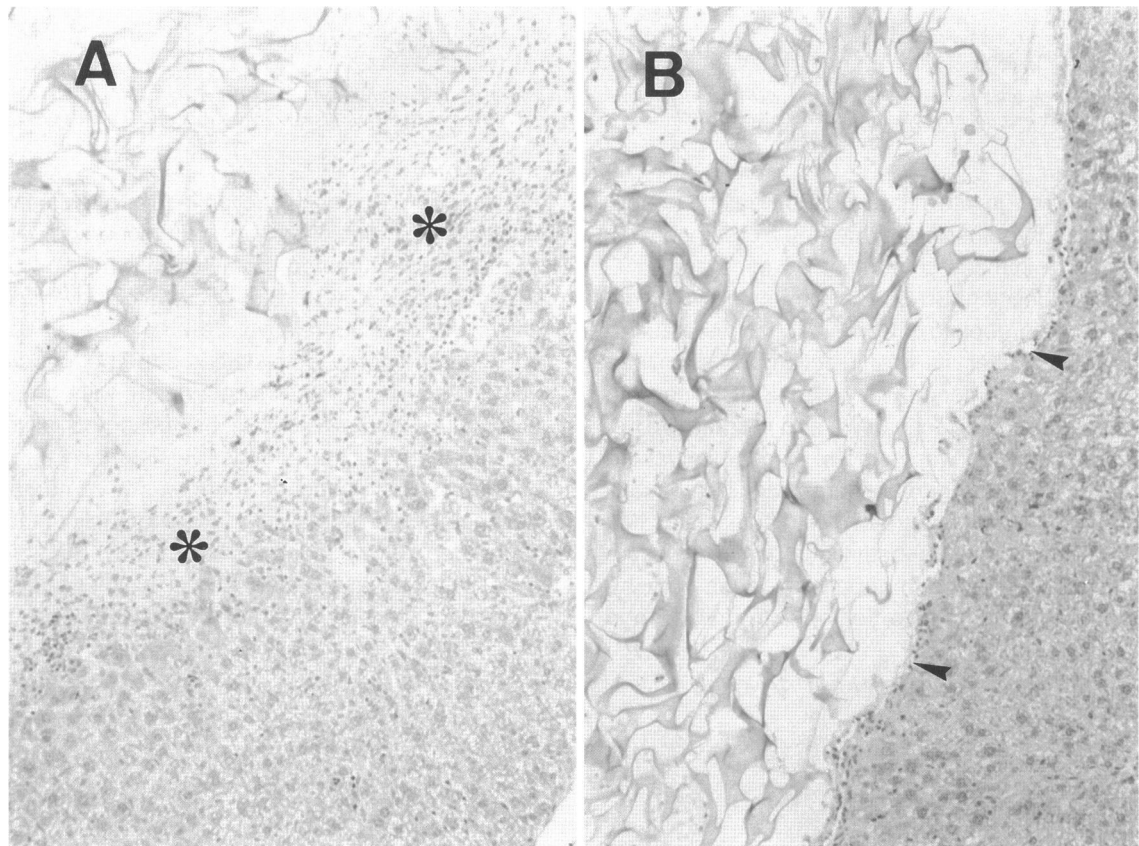


Figure 6. Interface between *rbFGFb* sponge/B16 melanoma liver implant and hepatic tissue (day 19) from *rmIL-12*- and pulse-*rhIL-2*-treated tumor-bearing B6 mice (A) or tumor-bearing B6 SCID mice depleted of NK cells (B). H&E; original magnification, $\times 66$. Sponges in both A and B are acellular. Note the minimal leukocyte infiltration at the sponge/liver interface in B6 SCID mice depleted of NK cells (B, arrowheads) as compared with immune-competent mice (A, asterisks).

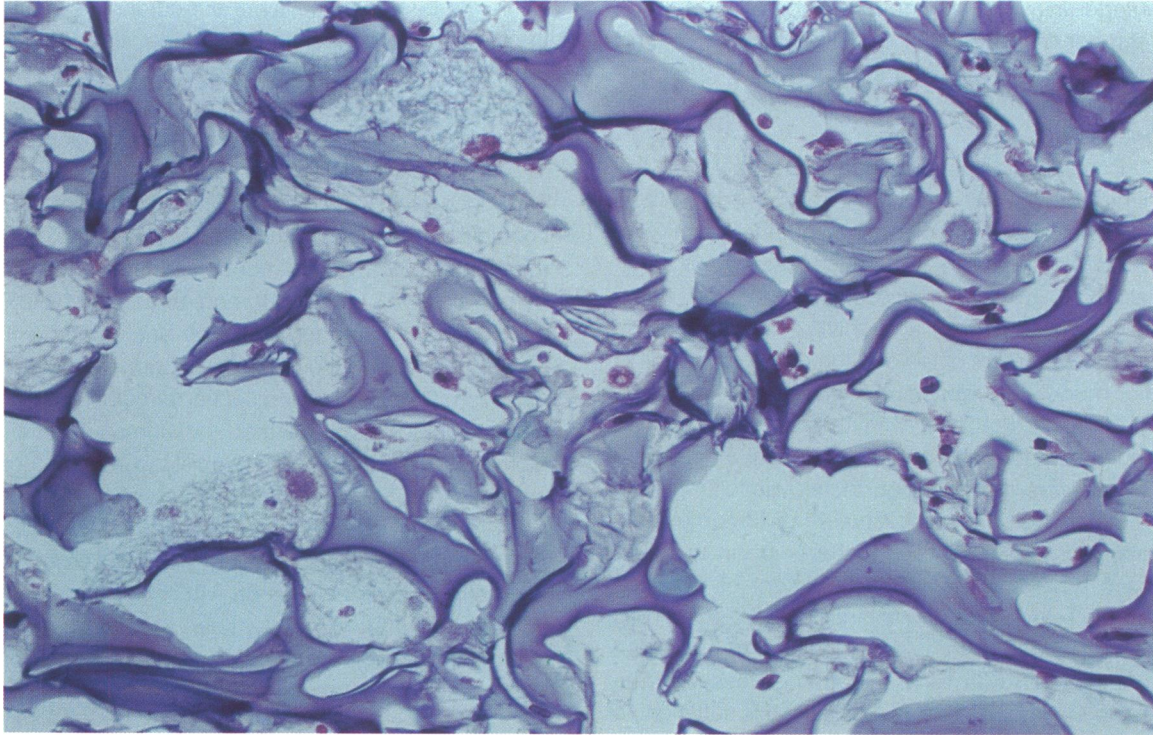


Figure 7. *rhFGFb sponge/B16 melanoma hepatic implant (day 19) from a B6 SCID mouse depleted of NK cells and treated with rmlL-12 and pulse rhIL-2. Masson's trichrome; original magnification, $\times 165$.*

mation of blood vessels at organ-specific sites.³³ Hepatic implantation of gelatin sponges containing rhFGFb resulted in a marked fibroblastic infiltrate 4 days after surgery, and in agreement with previous reports,^{32,33} blood vessels that had migrated away from the tissue site of implantation could be observed macroscopically within the gelatin sponge 2 weeks after implantation (Watanabe and Fogler, unpublished observation). In the absence of FGF, vascularization into the sponge does not occur.^{32,33} Although not investigated in the present study, the gelatin fibers of the sponge may also facilitate adhesion-mediated signals important for angiogenesis through newly recruited endothelial α_v integrins.³⁸ The sponge also served to provide a matrix to support the initial attachment and progressive growth of the B16F10 melanoma cell line. Occurring with growth of the tumor was a concomitant loss in the density of the gelatin fibers, presumably as a result of tumor-cell-elaborated protease digestion (Watanabe and Fogler, unpublished observation). The resulting pattern of tumor growth after sponge implantation onto the serosal surface of the left lateral hepatic lobe was a highly reproducible, localized lesion with hypervascular development, which eventually gave rise to peritoneal carcinomatosis.

To begin to investigate the utility of hepatic gelatin sponge implants containing FGF and tumor cells to

study the *in vivo* relationship between cytokine-induced leukocyte recruitment, angiogenic modulation, and anti-tumor activity, mice were treated with rmlL-12 and rhIL-2. Recent studies from our laboratory have shown that the combination regimen of rmlL-12 and rhIL-2 used in the current investigation induced a rapid and complete regression of primary and metastatic murine renal cell carcinoma (Renca) and displayed greater anti-tumor activity than that observed with either cytokine alone.³⁵ Results of that study suggested that both leukocyte-dependent and -independent mechanisms might play an important role in the anti-tumor activity of the rmlL-12 and rhIL-2 combination.³⁵ The parenteral injection of either IL-12 or IL-2 can induce profound effects on leukocyte recruitment and activation. In particular, either cytokine may enhance the proliferation, cytokine production, and cytotoxic activity of T lymphocytes and NK cells, and IL-12 or IL-2 can influence the development of a T-helper type 1 *versus* a T-helper type 2 pattern of cytokine production during the induction of an immune response.³⁹⁻⁴¹ Importantly, in addition to the immune-stimulating effects of IL-12, this cytokine has been shown to indirectly function as an antiangiogenic agent.^{42,43} The mechanism whereby IL-12 exerts its antiangiogenic effect is incompletely understood. However, it has been suggested that the process involves IL-12 induction

of interferon- γ with subsequent elaboration of IP-10, a member of the C-X-C chemokine family.^{42,43} This suggestion has been strengthened by the demonstration *in vivo* that IP-10 is a potent inhibitor of angiogenesis.²³

Our results in the current study show that the regimen of rmlL-12 in combination with rhIL-2 was effective against gelatin sponge implants of rhFGFb/B16F10 melanoma in SCID mice treated with anti-asialo-GM1 in the absence of a mononuclear infiltrate, suggesting that T and/or NK cells were not the principal mediators of the anti-tumor response in this tumor model. The absence of vascularity within the sponge after treatment with this specific cytokine combination suggested that a potential mechanism of action was the inhibition of neovascular growth associated with the establishment of tumor lesions. Preliminary experiments to further support this conclusion have shown that 1) treatment of B6 mice bearing 3-day hepatic implants of FGF-containing gelatin sponges (with no tumor cells) with pulse IL-2 in combination with IL-12 inhibits neovessel formation into the sponge and 2) IL-12 alone is sufficient to abrogate the vascular response and tumor growth when treatment is initiated 3 days after implantation of hepatic FGF sponges containing B16F10 melanoma into B6 *scid/scid* mice (data not shown). However, the relationship of these results to those reported by Wigginton et al,³⁵ where the combination regimen of IL-12 and IL-2 used in the current investigation induced a rapid and complete regression of primary and metastatic murine Renca and displayed greater anti-tumor activity than that observed with either cytokine alone, is not completely understood. Experiments are currently underway in our laboratory to further understand the relationship between the induction of leukocyte recruitment, angiogenic modulation, and anti-tumor activity after treatment of mice with pulse IL-2 and IL-12.

A number of salient features of this model deserve further comment. First, it is well recognized that organ-specific endothelium can express unique characteristics and either constitutive or cytokine-inducible ligands that are important for leukocyte adhesion and recruitment.⁴⁴⁻⁴⁶ It is also known that the neovasculature of progressively growing tumors and metastatic lesions can express traits associated with the pathological process that are distinct from the surrounding tissue.⁴⁷⁻⁴⁹ Gelatin sponge implants containing FGF have been used in our laboratory to generate cultures of organ-derived endothelial cells for *in vitro* investigations of leukocyte adhesion.³² The ability to implant sponges containing both tumor cells and an angiogenic stimulus to various organs

within the peritoneal cavity or subcutaneously offers the opportunity to investigate site-specific influences on *in vivo* tumor vasculature development^{50,51} and cytokine-induced leukocyte recruitment. This latter event can be studied by *in situ* immunohistochemistry or by FCA after disaggregation of the sponge. Second, gelatin sponge implants containing FGF should be amenable to study the *in vivo* pathological mechanisms that might control neovascularization by progressively growing tumors at a distant site. In this regard, this model would be analogous to the recently described mouse corneal pocket neovascularization assay used to discover circulating angiogenesis inhibitors generated by human tumors.²⁹ Moreover, we believe that the ability to implant these sponges onto target organs of metastatic disease, such as the liver, in a tumor-bearing host will allow the opportunity to also identify potential organ-derived effects on neovessel growth.^{50,51} Third, in contrast to the FGF-induced hypervascular response into gelatin sponges, the development and growth of hepatic sponge implants of B16F10 melanoma was not dependent on the presence of exogenous FGF. Both the B16F10 melanoma and the murine renal cell carcinoma line Renca form vascular tumors within the gelatin sponge matrix in the absence of FGF when implanted onto the liver or kidney, respectively, of syngeneic hosts (Watanabe and Fogler, unpublished observation). This finding would suggest that a tumor cell line expressing a transfected gene product thought to be involved in angiogenic modulation and/or leukocyte recruitment could be implanted within a sponge into various normal or genetically modified mouse recipient strains for the subsequent *in vivo* analyses of these processes. Finally, in the current studies, the incorporation of exogenous FGF into the sponge was used to induce a rapid, acute angiogenic response independent of tumor growth and to create a hypervascular tumor nodule to facilitate studies of leukocyte infiltration and angiogenic modulation. However, the autonomous growth and vascular development of hepatic sponge implants of B16F10 suggests that this model may also be useful to directly assess the influence of exogenous FGF and other proangiogenic growth factors on the *in situ* tumor-associated vascular expression of adhesion molecules believed important for leukocyte infiltration.^{18,47,49}

In summary, the model developed in the present study affords the opportunity to investigate the cellular and molecular mechanism(s) underlying both tumor angiogenesis and leukocyte recruitment. Ultimately, the experimental or clinical understanding of

this relationship should directly impact the treatment of metastatic tumor growth.

Acknowledgments

We thank the many individuals at Hoffmann-La Roche involved in the production and purification of the rmlL-12.

References

1. Folkman J: Angiogenesis in cancer, vascular, rheumatoid and other disease. *Nature Med* 1995, 1:27-31
2. Dvorak HF, Dvorak AM: Immunohistochemical characterization of inflammatory cells that infiltrate tumors. *Tumor Immunity in Prognosis: The Role of Mononuclear Cell Infiltration*. Edited by S Haskill. New York, Marcel Dekker, 1982, pp 279-302
3. Hogg N, Berlin C: Structure and function of adhesion receptors in leukocyte trafficking. *Immunol Today* 1995, 16:327-330
4. Carlos TM, Harlan JM: Leukocyte-endothelial adhesion molecules. *Blood* 1994, 84:2068-2101
5. Springer TA: Traffic signals for lymphocyte recirculation and leukocyte emigration: the multistep paradigm. *Cell* 1994, 76:301-314
6. Bevilacqua MP: Endothelial-leukocyte adhesion molecules. *Annu Rev Immunol* 1993, 11:767-804
7. Ben-Baruch A, Michiel DF, Oppenheim JJ: Signals and receptors involved in recruitment of inflammatory cells. *J Biol Chem* 1995, 270:11703-11706
8. DeVita VT, Hellman S, Rosenberg SA: *Biological Therapy of Cancer*. Philadelphia, JB Lippincott Co, 1995
9. Friesel RE, Maciag T: Molecular mechanisms of angiogenesis: fibroblast growth factor signal transduction. *FASEB J* 1995, 9:919-925
10. Burgess WH, Winkles JA: The fibroblast growth factor family: multifunctional regulators of cell proliferation. *Regulation of the Proliferation of Neoplastic Cells*. Edited by L Puzstai, CE Lewis, E Yap. Oxford, Oxford University Press, 1994, pp 155-218
11. Klagsbrun M, Soker S: VEGF/VPF: the angiogenesis factor found? *Curr Biol* 1993, 3:699-702
12. Dvorak HF, Brown LF, Detmar M, Dvorak AM: Vascular permeability factor/vascular endothelial growth factor, microvascular hyperpermeability, and angiogenesis. *Am J Pathol* 1995, 146:1029-1039
13. Claffey KP, Brown LF, Aguila LF del, Tognazzi K, Yeo K-T, Manseau J, Dvorak HF: Expression of vascular permeability factor/vascular endothelial growth factor by melanoma cells increases tumor growth, angiogenesis, and experimental metastasis. *Cancer Res* 1996, 56:172-181
14. O'Reilly MS, Holmgren L, Shing Y, Chen C, Rosenthal RA, Moses M, Lane WS, Cao Y, Sage EH, Folkman JA: Angiostatin: a novel angiogenesis inhibitor that mediates the suppression of metastases by a Lewis lung carcinoma. *Cell* 1994, 79:315-328
15. Volpert OV, Stellmach V, Bouck N: The modulation of thrombospondin and other naturally occurring inhibitors of angiogenesis during tumor progression. *Breast Cancer Res Treat* 1995, 36:119-126
16. Folkman J: Angiogenesis inhibitors generated by tumors. *Mol Med* 1995, 1:120-122
17. Koch AE, Halloran MM, Haskell CJ, Shah MR, Polverini PJ: Angiogenesis mediated by soluble forms of E-selectin and vascular cell adhesion molecule-1. *Nature* 1995, 376:517-519
18. Melder RJ, Koenig GC, Witwer BP, Safabakhsh N, Munn LL, Jain RK: During angiogenesis, vascular endothelial growth factor and basic fibroblast growth factor regulate natural killer cell adhesion to tumor endothelium. *Nature Med* 1996, 2:992-997
19. Strieter RM, Polverini PJ, Arenberg DA, Kunkel SL: The role of CXC chemokines as regulators of angiogenesis. *Shock* 1995, 4:155-160
20. Koch AE, Polverini PJ, Kunkel SL, Harlow LA, DiPietro LA, Elnor VM, Elnor SG, Strieter RM: Interleukin-8 (IL-8) as a macrophage-derived mediator of angiogenesis. *Science* 1992, 258:1798-1801
21. Strieter RM, Kunkel SL, Elnor VM, Martonyi CL, Koch AE, Polverini PJ, Elnor SG: Interleukin-8: a corneal factor that induces neovascularization. *Am J Pathol* 1992, 141:1279-1284
22. Cao Y, Chen C, Weatherbee JA, Tsang M, Folkman J: α - β , a -C-X-C- chemokine, is an angiogenesis inhibitor that suppresses the growth of Lewis lung carcinoma in mice. *J Exp Med* 1995, 182:2069-2077
23. Angiolillo AI, Sgadari C, Taub DD, Liao F, Farber JM, Maheshwari S, Kleinman HK, Reaman GH, Tosato G: Human interferon-inducible protein 10 is a potent inhibitor of angiogenesis *in vivo*. *J Exp Med* 1995, 182:155-162
24. Fogler WE, Volker K, McCormick KL, Watanabe M, Ortaldo JR, Wiltrout RH: NK cell distribution into lung, liver, and subcutaneous B16 melanoma is mediated by VCAM-1/VLA-4 interaction. *J Immunol* 1996, 156:4707-4714
25. Melder RJ, Salehi HA, Jain RK: Interaction of activated natural killer cells with normal and tumor vessels in cranial windows in mice. *Microvasc Res* 1995, 50:35-44
26. Melani C, Pupa SM, Stoppacciaro A, Menard S, Colnaghi MI, Parmiani G, Colombo MP: An *in vivo* model to compare human leukocyte infiltration in carcinoma xenografts producing different chemokines. *Int J Cancer* 1995, 62:572-578
27. Basse P, Herberman RB, Nannmark U, Johansson BR, Hokland M, Wasserman K, Goldfarb RH: Accumulation of adoptively transferred adherent lymphokine-activated killer cells in murine metastases. *J Exp Med* 1991, 174:479-488
28. Griffith KD, Read EJ, Carrasquillo JA, Carter CS, Yang JC, Fisher B, Aebersold P, Packard BS, Yu MY, Rosen-

- berg SA: *In vivo* distribution of adoptively transferred indium-111-labeled tumor infiltrating lymphocytes and peripheral blood lymphocytes in patients with metastatic melanoma. *J Natl Cancer Inst* 1989, 81:1709–1717
29. Chen C, Parangi S, Tolentino MJ, Folkman J: A strategy to discover circulating angiogenesis inhibitors generated by human tumors. *Cancer Res* 1995, 55:4230–4233
30. Kibbey MC, Corcoran ML, Wahl LM, Kleinman HK: Laminin SIKVAV peptide-induced angiogenesis *in vivo* is potentiated by neutrophils. *J Cell Physiol* 1994, 160:185–193
31. Pili R, Guo Y, Chang J, Nakanishi H, Martin GR, Passaniti A: Altered angiogenesis underlying age-dependent changes in tumor growth. *J Natl Cancer Inst* 1994, 86:1303–1314
32. MacPhee MJ, Wiltrout RH, McCormick KL, Sayers TJ, Pilaro AM: A method for obtaining and culturing large numbers of purified organ-derived murine endothelial cells. *J Leukocyte Biol* 1994, 55:467–475
33. Thompson JA, Anderson KD, DiPietro JM, Zwiebel JA, Zametta M, Anderson WF, Maciag T: Site-directed neovessel formation *in vivo*. *Science* 1988, 241:1349–1352
34. Park JA, Brown RA, Kurt RA, Akporiaye ET: Studies of *in vivo* recruitment and activation of cytotoxic lymphocytes using a gelatin-sponge model of concomitant tumor immunity. *Int J Cancer* 1995, 62:421–427
35. Wigginton JM, Komschlies KL, Back TC, Franco JL, Brunda MJ, Wiltrout RH: Administration of interleukin 12 with pulse interleukin 2 and the rapid and complete eradication of murine renal carcinoma. *J Natl Cancer Inst* 1996, 88:38–43
36. Pilaro AM, Taub DD, McCormick KL, Williams HM, Sayers TJ, Fogler WE, Wiltrout RH: TNF- α is a principal cytokine involved in the recruitment of NK cells to liver parenchyma. *J Immunol* 1994, 153:333–342
37. Watanabe H, Ohtsuka K, Kimura M, Ikarashi Y, Ohmori K, Kusumi A, Ohteki T, Seki S, Abo T: Details of an isolation method for hepatic lymphocytes in mice. *J Immunol Methods* 1992, 146:145–154
38. Friedlander M, Brooks PC, Shaffer RW, Kincaid CM, Varner JA, Cheres DA: Definition of two angiogenic pathways by distinct α_v integrins. *Science* 1995, 270:1500–1502
39. Lotze MT: Biologic therapy with interleukin-2: preclinical studies. *Biological Therapy of Cancer*. Edited by DeVita, S Hellman, SA Rosenberg. Philadelphia, JB Lippincott Co, 1995, pp 207–234
40. Trinchieri G: Interleukin-12: a proinflammatory cytokine with immunoregulatory functions that bridge innate resistance and antigen-specific adaptive immunity. *Annu Rev Immunol* 1995, 13:251–276
41. Magram J, Connaughton SE, Warriar RR, Carvajal DM, Wu C, Ferrante J, Stewart C, Sarmiento U, Faherty DA, Gately MK: IL-12-deficient mice are defective in IFN γ production and type 1 cytokine responses. *Immunity* 1996, 4:471–481
42. Voest EE, Kenyon BM, O'Reilly MS, Truitt G, D'Amato RJ, Folkman J: Inhibition of angiogenesis *in vivo* by interleukin 12. *J Natl Cancer Inst* 1995, 87:581–586
43. Sgadari, C, Angiolillo AL, Tosato G: Inhibition of angiogenesis by interleukin-12 is mediated by the interferon-inducible protein 10. *Blood* 1996, 87:3877–3882
44. Dahmen, U, Bergese SD, Qian S, Pelletier RP, Wu H, Sedmak DD, Fung JJ, Orosz CG: Patterns of inflammatory vascular endothelial changes in murine liver grafts. *Transplantation* 1995, 60:577–584
45. Bergese SD, Pelletier RP, Ohye RG, Vallera DA, Orosz CG: Treatment of mice with anti-CD3 mAb induces endothelial vascular cell adhesion molecule-1 expression. *Transplantation* 1994, 57:711–717
46. Pelletier RP, Morgan CJ, Sedmak DD, Miyake K, Kincaid PW, Ferguson RM, Orosz CG: Analysis of inflammatory endothelial changes, including VCAM-1 expression, in murine cardiac grafts. *Transplantation* 1993, 55:315–320
47. Wu NZ, Klitzman B, Dodge R, Dewhirst MW: Diminished leukocyte-endothelium interaction in tumor microvessels. *Cancer Res* 1992, 52:4265–4268
48. Nannmark U, Johansson BR, Bryant JL, Unger ML, Hokland ME, Goldfarb RH, Basse PH: Microvessel origin and distribution in pulmonary metastases of B16 melanoma: implication for adoptive immunotherapy. *Cancer Res* 55:4627–4632
49. Griffioen AW, Damen CA, Blijham GH, Groenewegen G: Tumor angiogenesis is accompanied by a decreased inflammatory response of tumor-associated endothelium. *Blood* 1996, 88:667–673
50. Fidler IJ: Modulation of the organ microenvironment for treatment of cancer metastasis. *J Natl Cancer Inst* 1995, 87:1588–1592
51. Fidler IJ, Ellis LM: The implications of angiogenesis for the biology and therapy of cancer metastasis. *Cell* 1994, 79:185–188